THE JOURNAL OF PHYSICAL CHEMISTRY B

ARTICLE

pubs.acs.org/JPCB

Dynamics of Ion Migration in Nanopores and the Effect of DNA−Ion Interaction

Shengting Cui

Department of Chemical and Biomolecular Engineering, University of Tennessee, Knoxville, Tennessee 37996-2200, United States

ABSTRACT: We have carried out Brownian dynamics calculations to investigate the effect of DNA−ion interaction on ion transport in a nanopore. We calculated the self-diffusion coefficient of monovalent ions in the presence of DNA in a nanopore and compared the result with that through an open pore, that is, without the presence of DNA. We find that the self-diffusion coefficient of the co-ions is essentially unaffected by the DNA. The self-diffusion coefficient of the counterions, on the other hand, is significantly reduced depending on the ion concentration. At high ion concentration, around 1 M, the effect of DNA on counterion diffusion is relatively small, causing a slight reduction in counterion diffusion coefficient. At low concentrations of a few millimolar, the effect is much larger, resulting in a reduction in counterion diffusion coefficient by a factor of about 2.5. The variation in the self-diffusion of the counterion is well described by accounting for the contributions from two components: the adsorbed counterions and the free counterions. Detailed dynamics of the DNA−counterion interaction is characterized by the varying length of the transient adsorption time of the counterions to the DNA charge sites and the exchange rate with the environment. This variation in counterion adsorption time is attributed to the ionic electric screening effect, which is in turn determined by the ion concentration.

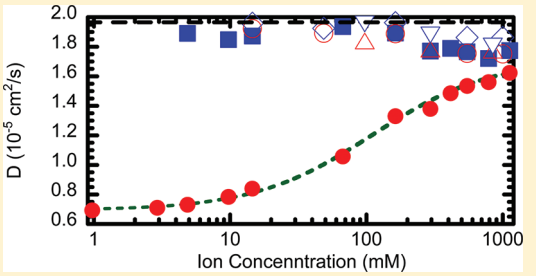

I. INTRODUCTION

Detection of a DNA-induced ionic current blockade has attracted considerable recent research interest,[1−9] as nanopores with diameter on the scale of ∼10 nm and smaller have been constructed. A number of recent works have reported experiments measuring the effect of DNA on ionic current through nanopores and the variation of such current with ion concentration.[6−9] A blockade current crossover from negative to positive has been observed as ion concentration is decreased, and the mechanisms of counterion condensation and volume exclusion have been invoked to describe the phenomenon with considerable success.[6−16] Fundamentally, the ionic flow involves two quantities: the ion concentration and the migration velocity of the ions. The physics of counterion condensation has been reasonably well understood, and the concept of volume exclusion can be intuitively understood. In comparison, our understanding of the dynamic process of ion migration in nanopores when DNA is present is still very limited. A complicating factor in the quantitative analysis of the ion migration is that the counterions are only transiently adsorbed to the DNA (at the charge sites) with an adsorption time on the order of nanoseconds.[17] On a macroscopic time scale, numerous association−dissociation events take place, and the counterions adsorbed to the DNA cannot be treated as static. Thus, there is no straightforward way to account for the effect of the transiently adsorbed counterion. In addition, there is a lack of knowledge of the detailed dynamics of how an initially free counterion becomes adsorbed to DNA and of the associated exchange process between an adsorbed and a free counterion. Furthermore, the DNA−ion interaction is attenuated by the presence of background ions. Classical theory has suggested the important effect of the background ions, through electric screening, as characterized by the well-known Debye length, which is determined by the ion concentration.[18−20] It is thus expected that counterion migration in the presence of DNA should significantly depend on the ion concentration. Therefore, a good understanding of the mechanism of the DNA−counterion interaction in nanopores, its effect on the ion migration, and the dynamics of the counterion dissociation−association is needed for future practical effort in the field.

Theoretical and modeling studies of DNA have been performed using a variety of approaches including analytical theory, coarse grained approaches such as Poisson−Boltzmann (PB) calculations and Brownian dynamics (BD), and fully detailed atomistic molecular dynamics simulations. The DNA counterion condensation theory originated with Manning's theoretical analysis on a simple line charge model. It predicts a critical line charge density above which the system becomes unstable and counterions condense to the line charge to reduce the effective line charge density to a stable value.[10,21] Electrostatic approaches, in which the solvent is treated as a continuum, have been used in the study of DNA packaging in viruses, bacteria, and chromosomes, and they have been used to investigate the underlying mechanism—counterion induced DNA−DNA attraction.[22−25] Similarly, electrostatic approaches have been used to study protein structures

Received: November 21, 2010
Revised: July 7, 2011
Published: July 29, 2011

dx.doi.org/10.1021/jp111111u | J. Phys. Chem. B 2011, 115, 10699–10706

Table 1. Potential Models and Parameters Used in the Simulation[a]

interaction pair	ε (kcal mol^{-1})	σ (Å)	q (e)	D (10^{-5} cm^2/s)	μ (10^{-4} cm^2/(V s))
K^+ [b]	0.1000	3.332	+1	1.957	7.616
Cl^- [b]	0.1000	4.400	−1	2.032	7.909
K^+—wall[c]	0.1520	3.166			
Cl^-—wall[c]	0.1520	3.700			
DNA charge sites[d]	0.1520	3.200			
DNA core[e,f]	0.1520	3.200			

[a] ε and σ are the Lennard-Jones energy and size parameters, q is electric charge, and D and μ are the self-diffusion coefficient and mobility at infinite dilution, respectively. [b] Ion—ion interaction, WCA potential: $V(r) = 4\varepsilon\{[(\sigma/r)^{12} - (\sigma/r)^6] - [(\sigma/r_{cut})^{12} - (\sigma/r_{cut})^6]\}$. The Lorentz—Berthelot combining rule is used for cross-interaction. [c] Ion—wall interaction: $V(r) = 4\varepsilon(\sigma/r)^{12}$, $r = (R - \rho)$, where R is the pore radius, and ρ is the radial distance of the ion. [d] Ion—DNA charge site interaction, WCA potential; Lorentz—Berthelot combining rule for the interaction. [e] Ion—DNA core interaction (cylindrical portion): $V(r) = \varepsilon(\sigma/r)^{12}$, $r = \rho - r_0$, where ρ is the radial distance of the ions from the DNA center axis and r_0 = 8 Å is the core radius of the DNA. [f] Ion—DNA core interaction (caps): $V(\rho) = \varepsilon(\sigma/\rho)^{12}$, $\rho = |r| - r_0$, $\boldsymbol{r} = \boldsymbol{r}' - \boldsymbol{r}_\pm$, where $\boldsymbol{r}'$ and $\boldsymbol{r}_\pm$ are the position vectors of the ion and the centers of the semispherical end-caps of the DNA, respectively, and ρ is the distance from the cap surface to the ion.

and protein—protein interactions.[26] In recent years, molecular dynamics has increasingly been used to study DNA. A number of studies have investigated the DNA—ion interaction in bulk aqueous solution.[27−30] Because of the important potential in nanopore based DNA sequence detection, behaviors of DNA within the nanopore environment are being intensely investigated[31−35] (see ref 35 for a review on the subject). These investigations have significantly advanced our understanding of the DNA—ion interaction.

In this study, we carried out a Brownian dynamics simulation study to obtain a detailed understanding of the microscopic mechanisms for ion migration in nanopores in the presence of DNA. We investigated the diffusive migration of monovalent counterions and co-ions and the dynamics of counterion adsorption to the DNA, as characterized by the residence time correlation functions (RTCF) of the counterions to the charge sites of the DNA. We further analyzed the effect of the adsorption dynamics on the diffusion of the counterions and the role of the electric screening in modulating DNA—ion interaction and, hence, its migration. In the following, we present our methods and results. We discuss and analyze the results to elucidate our understanding of the microscopic mechanisms of ion transport in nanopores.

II. MODELS AND METHODS

We carried out a Brownian dynamics study of dsDNA in nanopores with K^+ and Cl^- ions for a range of ion concentrations. In our system, the dsDNA is fixed in space. Only the ions undergo Brownian motion. The equation of motion for the ions is given by the following:[36,37]

$$m_i \frac{d\mathbf{v}_i}{dt} = \mathbf{f}_i - \zeta_i \mathbf{v}_i + \mathbf{f}_i^R \quad (1)$$

where m_i is the mass of the ion (labeled with index i), $\mathbf{v}_i$ is the instantaneous velocity vector, $\zeta_i = k_B T/m_i D_i$ is the friction coefficient with D_i as the self-diffusion coefficient in bulk fluid at infinite dilution, k_B is the Boltzmann constant, and T is the temperature. $\mathbf{f}_i$ is the force due to other ions, DNA, and the pore, and $\mathbf{f}_i^R$ is the random Brownian force representing the effect of the solvent. The position and velocity are updated using the standard algorithm.[38] DNA is treated as immobile, as its thermal velocity is negligible compared to that of the ions.[16]

In our calculations, the DNA is modeled as a straight cylinder with an exclusive core radius of 0.80 nm. Negative charges of $-e$ each are placed 0.3 nm out from the core surface in a double-helical arrangement. The DNA is capped with hemispherical caps of 0.80 nm at both ends.[25] The total length of the pore is 21.76 nm, and the diameter is 10 nm. The DNA is placed at the center of the pore and is parallel to the axis of the pore. The DNA length considered here is less than the persistence length of the double-stranded DNA (∼50 nm) and is intended to represent a short segment of a long dsDNA, which should be reasonably straight. The total length of the DNA (including the hemispherical caps) is equal to the nanopore length, with the cylindrical portion carrying 114 units of electric charges. The K^+ and Cl^- interact with the DNA and with each other through a soft sphere potential and electrostatic interaction.[39] The soft sphere interaction potentials and relevant parameters used in this study are summarized in Table 1. The dielectric constant of the media far from the DNA in the radial direction is 78.4, modeling an aqueous environment. Close to the surface of the DNA, it has been recognized that the dielectric constant varies with the distance from the DNA.[40−42] We have thus used a distance dependent dielectric constant within 1 nm from the surface of the DNA, derived on the basis of a fitting to the local dielectric constant obtained from molecular dynamics simulation.[40] It is given in mathematical form as $\varepsilon_\epsilon(r) = \varepsilon_0 - [((\varepsilon_0 - \varepsilon_i)/2)(\alpha^2 + 2\alpha + 2)e^{-\alpha}]$, where $\alpha = sr$; $s = 1.2$ Å^{-1}; $\varepsilon_0 = 78.4$; $\varepsilon_i = 1.76$; and r is the distance from the DNA surface. For $r > 1$ nm, $\varepsilon_\epsilon(r)$ is indistinguishable from ε_0. Because the focus of the study is to investigate the effect of the DNA—ion interaction on the diffusion of the ions, we have chosen to model the nanopore wall as neutral, so that there is no electric effect on the diffusion of the ions from the wall and all the effects are solely due to the DNA. In many experimental situations, the nanopore wall may be charged. We have shown in a previous study that the major effect of such electrically charged walls is the enhancement of the electric double layer overlap when DNA enters the pore, causing the ionic concentration in the pore to deviate from that without DNA. For simplicity in this study, we are using a neutral wall in order to isolate the effect of the DNA from that of the wall on the ion diffusion. For cases of electrically charged walls, the ion concentration used here should be considered an equivalent concentration (after taking into account the electric double layer overlap effect).

Our main interest is in the system where the nanopores are sufficiently large so that a continuum picture for the solvent is applicable. Thus, we have chosen a pore size of 10 nm in diameter (except Section III.4 where we study the effect of pore size), which is about 30 times larger than the size of a water molecule, ∼0.3 nm. In addition, we have neglected the desolvation effect due to the molecular nature of the water molecules, which has been found to be important for small pores ∼2 nm.[43,44]

The electrostatic long-range interaction is treated as it was in our previous publication.[45] Because of the one-dimension nature

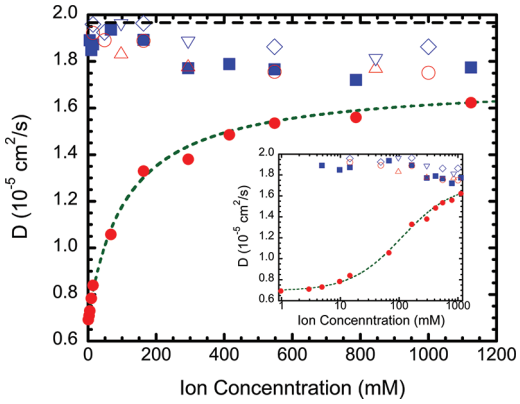

Figure 1. Diffusion coefficient for ions in the nanopore in the presence and absence of DNA as a function of ion concentration. Horizontal dashed line, infinite dilution limit for K^+ in the bulk solution; solid circles, K^+ in the presence of DNA; solid squares, Cl^- in the presence of DNA; open circles, K^+ in the open pore; open diamonds, Cl^- in the open pore; upward facing triangles, K^+ in the presence of the hard core cylinder; inverted triangles, Cl^- in the presence of the hard core cylinder; and dashed line, eq 2b (with $D_{ads} = 0.693 \times 10^{-5}$ cm^2/s and $D_{free} = 1.715 \times 10^{-5}$ cm^2/s). The inset displays the same plots on a logarithmic scale of ion concentration to show the approach to a plateau at low ion concentration.

of the system at large distances and the electric neutrality of the system, the long-range correction to the electrostatic interaction can be integrated to give an analytic expression of the line-charge method approach.[46]

The total number of ions in our systems ranges from 116 to 2430. The time step used for updating the position and velocity of the ions is 0.0252 ps. Typical calculations run for 5 to 30 million time steps, depending on the ion concentration. In an extreme case at low concentration, we have run the calculation as long as 200 million time steps.

III. RESULTS

III.1. Dependence of Counterion Self-Diffusion on Ion Concentration. The diffusion coefficients for K^+ and Cl^- in the axial direction are calculated using the Einstein relation, $\langle[\mathbf{r}_{||}(t) - \mathbf{r}_{||}(0)]^2\rangle = 2D_{||}t$, where the symbol $||$ is used to denote the direction parallel to the pore axis. We note that the diffusion coefficient obtained here does not include the effect of hydrodynamic interaction. In general, the calculation of dynamic properties should take into account the hydrodynamic interaction.[47] For the self-diffusion coefficient of small ions, however, it has been shown[48−50] that the effect of the hydrodynamic interaction is less than about ∼3% at the highest ion concentration studied here and negligible below 300 mM; therefore, the hydrodynamc interaction would not affect the discussion below.

The calculated diffusion coefficients vs ion concentration (in this work, the ion concentration in the nanopore is defined as the concentration of the co-ions) are plotted in Figure 1. The most striking feature is that, in the presence of DNA, the diffusion coefficient for the counterion decreases with the decreasing ion concentration, essentially approaching a plateau at very low ion concentration. At the lowest concentration studied, where the Cl^- concentration is 1 mM, the K^+ diffusion coefficient had decreased to about 40% of the value at the highest concentration studied, about 1.125 M. On the other hand, the variation in co-ion diffusion coefficient is much smaller, increasing slightly with the decreasing ion concentration and tending toward the dilute solution limit, 2.032×10^{-5} cm^2/s.[51] This slight increase is obviously due to the less frequent collisions among ions at lower concentration. For comparison, we also plot the results for ion diffusion in an open pore where there is no effect caused by DNA. It is seen clearly that, for an open pore, both the counterion and the co-ion diffusion coefficients show similar trends, slightly increasing with decreasing ion concentration. The horizontal dashed line in Figure 1 shows the experimental K^+ diffusion coefficient at infinite dilution, 1.957×10^{-5} cm^2/s, as a reference.[51] The presence of the DNA clearly has an important effect on the dynamics of the counterion transport in the nanopore. A similar effect has been found in NMR measurements of Li^+ and Cs^+ diffusion in humidified DNA fibers, where a reduced counterion diffusion coefficient compared to bulk fluid, as well as a decrease with decreasing salt concentration, were observed.[52]

Physically, we understand that, at the few lowest ion concentrations studied here, there are very few co-ions. The vast majority of ions are counterions, which are necessarily present to electrically neutralize the charges of the DNA so that the system as a whole is electrically neutral. In the extreme case, the co-ion concentration is so low that the ratio of the total DNA charge and total counterion charge is nearly unity; the attractive interaction between the counterions and the DNA reaches maximum strength absent of the mediating effect of the co-ions, so the diffusion coefficient approaches a plateau. On the other hand, at the highest ion concentration studied here, the ratio of the number of DNA charges to the total number of counterions is about 9%, so the counterion diffusion is largely dominated by the contribution from the free counterions.

Note that the diffusion coefficient is calculated as an average over all the counterions or co-ions because it is impossible to separate the adsorbed and free counterions, as the same ion can dynamically change roles from being adsorbed to being free and vice versa (see Sections III.2 and III.3 for more details). To better quantitatively understand the counterion diffusion slowing down by the DNA, we decompose the contribution to the average diffusion coefficient into the components resulting from adsorbed and free counterions as follows:

$$D_{eff} = \frac{1}{N^+}[D_{ads}N_{DNA} + D_{free}(N^+ - N_{DNA})] \qquad (2a)$$

where D_{eff} ($D_{eff} = D_{||}$ of the Einstein relation) is the effective average diffusion coefficient over all counterions in the nanopore; D_{ads} corresponds to the plateau diffusion coefficient of the adsorbed counterions at very dilute ion concentration ($D_{ads} = 0.693 \times 10^{-5}$ cm^2/s is the counterion diffusion coefficient at 1 mM. See the inset of Figure 1); D_{free} is the diffusion coefficient of the free counterions ($D_{free} = 1.715 \times 10^{-5}$ cm^2/s, derived by extrapolation to high concentration on the basis of the simulation data); N^+ is the total number of counterions; and N_{DNA} is the number of charge sites on the DNA. Note that $N^+ = N^- + N_{DNA}$, where N^- is the number of co-ions. Because the ionic number appears in both the denominator and numerator, eq 2a is a nonlinear function of the ionic numbers. The physical significance of a nonzero D_{ads} is that although we need N_{DNA} counterions to completely neutralize the DNA charge in the nanopore, there is always a fraction of counterions at any instance of time which remain free as a result of the incomplete physical adsorption of the counterions to the DNA, unlike in the stronger chemical adsorption. The adsorbed counterions can occasionally dissociate from

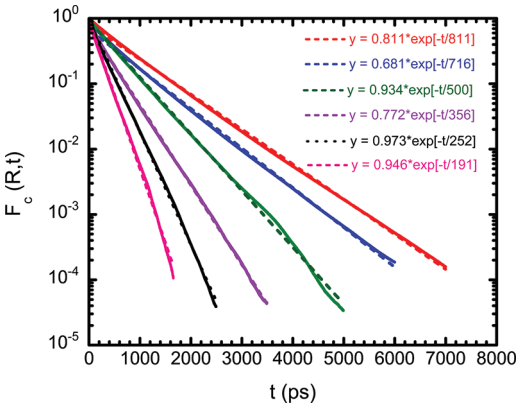

Figure 2. Continuous residence time correlation functions (RTCF) for various ion concentrations. Color code: red (1 mM), blue (15 mM), green (67 mM), purple (294 mM), black (548 mM), and pink (787 mM). The decrease in the residence time implies the faster decay of the RTCF with time as the ion concentration increases from 1 to 787 mM.

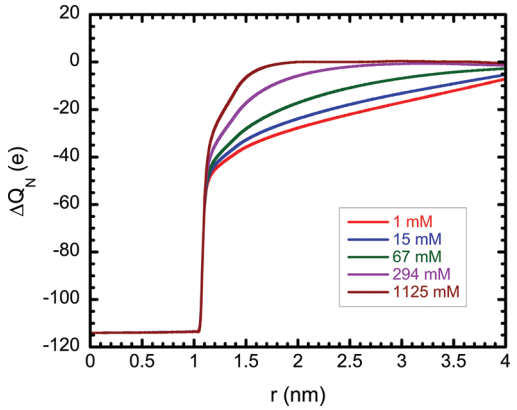

Figure 3. Total charge around the DNA in the nanopore within a cylindrical volume of radial distance less than r, $\Delta Q_N = \Sigma_i q_i^+ + \Sigma_j q_j^- + Q_{DNA}$ as a function of r. The deviation of ΔQ_N from zero signifies a deviation from charge neutrality within the volume.

the DNA and become free and vice versa. The result is plotted as the short-dashed line in Figure 1. It is seen that this simple two-component analysis describes very well the concentration dependence of the diffusion coefficient for the counterions in the nanopore in the presence of DNA. Thus, for conceptual convenience, the diffusion of the counterions in the presence of DNA can be attributed to two contributions: one from adsorbed counterions with a reduced diffusion coefficient and the other from free diffusing counterions.

For practical purposes, it is useful to recast eq 2a in terms of concentrations instead of the number of ions and charge sites. This can be done by dividing both the numerator and denominator by the volume, resulting in the following:

$$D_{eff} = \frac{1}{C^+}[D_{ads} C_{DNA} + D_{free}(C^+ - C_{DNA})] \quad (2b)$$

where C^+ and C_{DNA} are the concentrations of the counterions and the DNA charge sites in the nanopore, respectively. Note that the ion concentration appears in eq 2b implicitly through the relation $C^+ = C + C_{DNA}$ as a result of the charge neutrality in the nanopore.

III.2. Dynamics of Counterion Dissociation from DNA. To gain a deeper understanding of the effect of DNA−ion attraction on the mobility of the counterions, we calculated the continuous residence time correlation function (RTCF) of the counterions around a DNA charge site, defined as[53,54]

$$F_c(R,t) = \frac{\sum_{i,j} \langle \theta_{ij}(R,0)\, \theta_{ij}(R,t) \rangle}{\sum_{i,j} \langle \theta_{ij}(R,0)\, \theta_{ij}(R,0) \rangle} \quad (3)$$

where the double summation is over all charge sites of the DNA, i, and all the counterions, j. $\theta_{ij}(R,t)$ is the Heaviside step function, which is 1 if a counterion remains continuously within a radial distance R of a DNA charge site, taken to be twice the van der Waals diameter of the potassium ion and DNA interaction, $R = (R_i + R_{DNA}) = 7.332$ Å, from time 0 to t, and 0 otherwise, where $R_i = 2^{1/6}\sigma_i$, and $R_{DNA} = 2^{1/6}\sigma_{DNA}$ are the van der Waals diameters of the ion and the DNA charge site, respectively (see Table 1). The angular brackets represent a time average from the BD simulation. Equation 3 defines a correlation function at time t for the fraction of counterions that were within the radial distance R of a DNA charge at time 0 and that have never left the spherical volume within R in the time interval $[0, t]$. It can be reasoned that if a counterion spends a considerable amount of time around a DNA charge site, its migration would then be substantially delayed, resulting in a lower mobility.

The results are shown in Figure 2 for a range of ion concentrations. It is seen that the RTCF closely follow an exponential form, with characteristic times depending on the ion concentration. By fitting the RTCF to the exponential function, we derive a characteristic residence time corresponding to each ion concentration, obtaining values for the residence time, t_R = 811, 716, 500, 356, 252, and 191 ps for ion concentrations 1, 15, 67, 294, 548, and 787 mM, respectively. The results show that the residence time strongly depends on the ionic concentration, decreasing with increasing ion concentration. At the lowest concentration, 1 mM, the co-ion population is less than 1% of the counterion population in the nanopore that is needed to neutralize the negative charges on the DNA. As a result, the interactions between the counterions and the DNA charge are essentially the unscreened bare interactions; so, the counterions experience the strongest attraction by the DNA. It is thus more difficult for them to escape from the DNA, resulting in a long residence time. Inversely, as the ion concentration increases, there are a large proportion of background ions that are not directly adsorbed to DNA charge sites but rather are spread throughout the nanopore at all radial distances. These ions are more or less free to move about in the pore in response to the local electric field to reduce the interaction strength, such as that between the DNA and the counterions. Furthermore, as a result of the abundant presence of the background ions, exchanges of the free counterions with the adsorbed counterions are more readily possible, so the exchange events occur more often; this, in effect, also contributes to the shortening of the residence time of the adsorbed ions.

In the theory of ionic solutions,[18−20] the electric potential from a charge Q is given, apart from a constant prefactor, by $Qe^{-r/\lambda_D}/r$, where r is the distance from the charge and λ_D is the Debye length, given (in SI units) by $\lambda_D = (k_B T \varepsilon_e / e^2 c_s)^{1/2}$ for monovalent ionic solution, where k_B is the Boltzmann constant, T is the temperature, ε_e is the dielectric constant, e is the

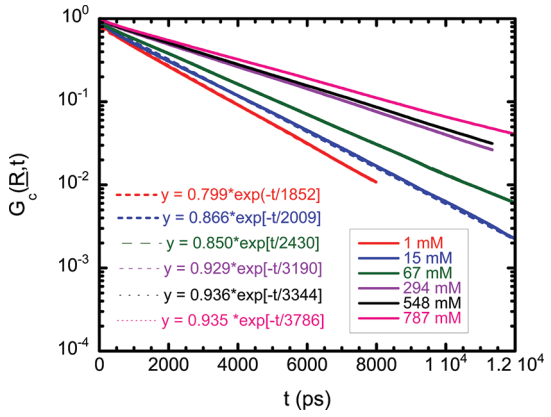

Figure 4. Continuous residence time correlation function (RTCF) for a counterion to stay outside the influence sphere of the DNA charges, during which time the counterions undergo uninterrupted free diffusion without being transiently adsorbed to the DNA. The color code is the same as that for Figure 2.

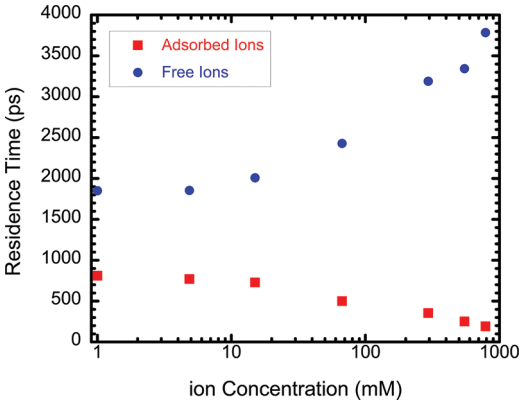

Figure 5. Concentration dependence of the residence times for the adsorbed counterions and free counterions.

magnitude of electron charge, and c_s is the total number density of the ions. Beyond the distance λ_D, the effect of the charged object is largely neutralized by the opposite charged ions. Thus, an effective manifestation of the electric screening is the charge neutralization around the DNA by the small mobile ions. This is shown in Figure 3, where the net electric charge within a certain distance r in the radial direction, ΔQ_N, including K^+, Cl^-, and those of DNA ($\Delta Q_N = \Sigma_i q_i^+ + \Sigma_j q_j^- + Q_{DNA}$) are plotted. Clearly, the electric neutrality varies with the ion concentration. At the two lowest ion concentrations shown, 1 and 15 mM, the charge neutrality is not reached until the nanopore wall. As the ion concentration increases, DNA charges are increasingly better screened. At 294 mM, DNA charges are essentially completely screened at 2 nm from the DNA surface (which is at $r \approx 1$ nm). At 1125 mM, the DNA charge is completely screened by the counterions about 1 nm from the DNA surface. The rapid initial rise of the plots near $r = 1$ nm in the figure is due to the counterions directly bound to the DNA. At an intermediate distance from the DNA (1.2−1.5 nm), the net charge also increases faster with the ion concentration. The net effect of this concentration-dependent electric screening (or the lack of) is the weaker DNA−counterion attraction at high ion concentration, or inversely, stronger DNA−counterion interaction at low ion concentration. This results in longer residence time for the counterions, which in turn leads to slower migration.

III.3. Dynamics of Free Counterion Adsorption to DNA. Similar to the function $F_c(R, t)$, we can define the correlation function $G_c(\underline{R}, t)$, which describes a counterion initially in the region $\underline{R}$ complementary to the region R in the nanopore (here, R is a combination of spherical volumes within a specified distance R for all DNA charge sites, and $\underline{R}$ spans the whole region in the nanopore exclusive of R) and continuously stays in region $\underline{R}$ until it enters into a local spherical volume associated with one of the DNA charge sites. In Figure 4, we show the correlation function $G_c(\underline{R}, t)$ for a range of concentrations from 1 to 787 mM.

It is seen that as the ion concentration increases, the residence time for the ions to stay away from the DNA becomes longer, ranging from 1852 to 3786 ps for the range of ion concentrations studied. The increase in free ion residence time with ion concentration is mainly due to two factors. One is that as the ion concentration increases, the electric screening causes the attractive interaction between the DNA charges and the counterions to weaken so that the counterions are less likely to be attracted to the DNA. The other is that as the ion concentration increases, the free counterions are more abundant so that, on average, the probability is smaller for each counterion to come into close encounter with a charge site of the DNA. Compared with the residence time of the counterions to remain adsorbed to the DNA, the time duration for the counterions to stay free is significantly larger. At the highest ion concentration calculated for $G_c(\underline{R}, t)$, 787 mM, the time duration for the counterions to stay free is more than an order of magnitude larger than the bound counterion residence time, which suggests that, at high ion concentration, a counterion initially unbound to the DNA can migrate freely with relatively little interference from the DNA. Thus, at high concentration, the counterion diffusion coefficient eventually tends toward the open pore limit.

It is also noted that the residence time for adsorbed and free counterions varies with ion concentration with the opposite trend, which is shown in Figure 5. The difference between the adsorbed and the free counterion residence times narrows as the ion concentration decreases. At 1 mM ion concentration, the difference is only about a factor of 2 between the free and the bound counterions; so, the counterion transport at low ion concentration is characterized by an intermittent process in which the free counterion migration is frequently interrupted by DNA charges that momentarily trap the counterions to a particular charge site. At a very low ion concentration, the residence times of both the adsorbed and free counterions approach plateaus, consistent with the same behavior for the diffusion coefficient.

The results in Figure 5 show that for the nanopore size studied here the free counterion residence time is always larger than the bound counterion residence time. It is possible, however, that as the nanopore diameter decreases, the free counterion residence time may decrease and becomes similar to or even smaller than the bound counterion residence time. As a result, the counterion migration through the nanopore will be more severely reduced.

III.4. Effect of Pore Size on Counterion Residence Time. To further elucidate the exchange dynamics between free and adsorbed counterions, we investigate the dependence of residence times on the diameter of the pore. For simplicity in comparison, we keep the ion concentration constant while varying the pore diameter. In Figure 6, we plot the residence time of the adsorbed and free counterions as a function of pore diameter for ion concentration 67 mM. It is seen that, in the range of pore size

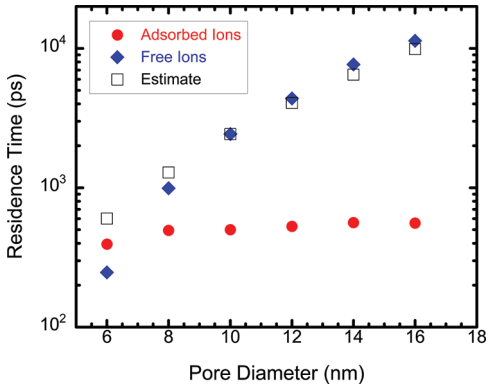

Figure 6. Counterion residence time as a function of pore diameter. The solid symbols are from the simulation, and the open squares represent the estimate based on scaling eq 4.

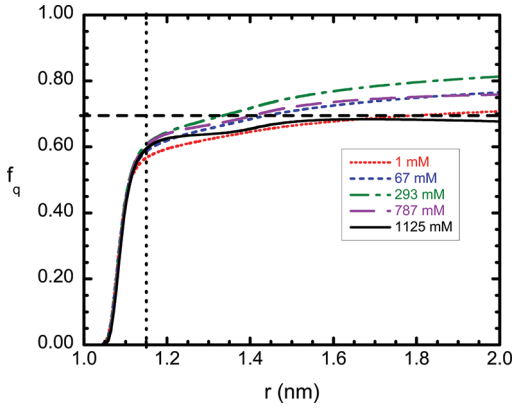

Figure 7. Fractional counterion condensation to the DNA as a ratio between the excess number of counterions to the total number of DNA charge sites as a function of radial distance.

studied, the residence times of the bound counterions vary only slightly, except for the smallest diameter, where a large drop is observed, whereas that of the free counterion residence time varies by an order of magnitude. In the plot, the data labeled "estimate" for the free counterion residence time are obtained from the following scaling equation, using the calculated value of the residence time for the 10 nm pore as a reference point.

$$\tau_d^f = (V_d^f/V_{10}^f)\left(\frac{N_d^+}{N_{\mathrm{DNA}}}/\frac{N_{10}^+}{N_{\mathrm{DNA}}}\right)\tau_{10}^f$$

$$= (V_d^f/V_{10}^f)(N_d^+/N_{10}^+)\tau_{10}^f \qquad (4)$$

where τ_d^f, V_d^f, and N_d^+ are the residence time, the spatial volume of free counterions in the nanopore excluding the volume of the DNA, and the total number of counterions in a nanopore of diameter d, respectively. The subscript 10 implies that d is set equal to 10 nm, which is the reference pore size for the scaling. N_{DNA} is the number of charge sites on the DNA, as before.

For the bound counterions, the behavior of the residence time is relatively easy to understand, as it is largely determined by the local interactions between the DNA charge sites and counterions. For the free counterions, there are two dominant determining factors. One is the available spatial volume for the free counterions, which varies quadratically with pore diameter. This translates into a phase space volume for the free counterions to explore. The second is that there are more counterions than can be adsorbed by the DNA, so there is a permutation process for different counterions to be adsorbed to DNA through adsorbed−free counterion exchange. The more counterions, the longer the permutation takes. This prolongs the time for the rest of the counterions to remain free. The fact that the estimated free counterion residence time using eq 4 gives values in close agreement with those from the simulation for an order of magnitude variation suggests the correctness of the suggested mechanism here.

The reason for the steep drop at smallest pore diameter is that as the free counterions' phase volume decreases, they not only have a small phase volume but are also closer to the DNA because of the confinement; thus, they are more strongly attracted by the DNA. As a result, the time duration for them to remain free is shortened more than is described by eq 4, as seen in Figure 6. This also leads to more frequent exchanges with the bound counterions to reduce the bound counterion residence time. However, the total cumulative time that the counterions stay bound to the DNA is longer, so this should have the effect of reducing the diffusion rate of the counterions through the nanopore. We caution that, for the smallest pore of 6 nm in diameter, there might be some explicit solvent effect; thus, a full atomistic simulation may be needed to more accurately quantify the process. Though on physical ground, we can easily understand the qualitative trend. Another effect for the small nanopore is the strong co-ion depletion by DNA that has been discussed in a prior work.[17]

III.5. Counterion Condensation to DNA in Nanopore. To better understand counterion transport, it is also useful to have some knowledge about the amount of counterions attracted to the DNA, commonly referred to as the counterion condensation. In this study, we characterize it by f_q, the fraction of DNA charge that is counterbalanced by the adsorbed counterions. For this purpose, we calculated the excess number of counterions around the DNA as a fraction of charge on the DNA. This is obtained by subtracting the background contribution in the region sufficiently far away from the DNA in the radial direction (at 3 nm). In Figure 7, we show such excess charges as a fraction of the total DNA charge, which falls between about 0.60 and 0.82, with small variation between the radial distance 1.1 and 2.0 nm. For $1.05 \leq r \leq 1.15$ nm, f_q quickly rises to about 0.60, a value which is fairly insensitive to the ion concentration. This rise at short distance is obviously due to the counterions that are more tightly bound to the DNA charge sites and are relatively immobile. They neutralize about 60% of the charges on DNA. Further away, there is a gradual, slow rise of values to between about 0.68 and 0.82. These account for the counterions that are weakly attracted to the DNA, and their motion is relatively more mobile than that of the tightly bound counterions. Molecular dynamics simulations have been performed to study ion distribution around DNA,[27,29,33] from which the fraction of DNA charge neutralized was determined. Values between 0.72 and 0.75[33] and 0.76[27,29] have been obtained, with some variation in the Manning radius used. The results obtained here are comparable to these studies. Early experiments based on NMR and electrophoresis measurements reported values for the fractional counterion condensation in the range 0.53−0.85.[10−14] An optical tweezers experiment reported the value 0.75.[15] However, the result has been reinterpreted by theoretical analyses,[55,56] and a molecular dynamics study by Aksimentiev et al.[33] has provided detailed mechanisms and interpretation on

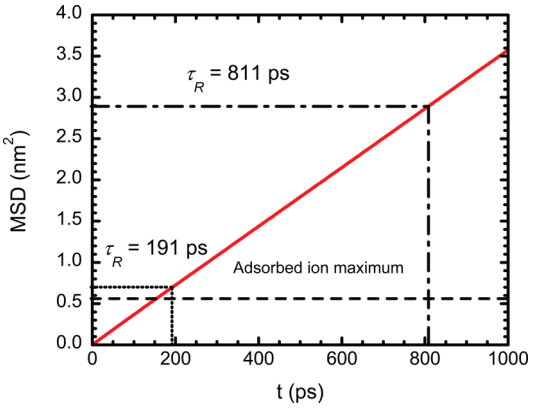

Figure 8. Effect of counterion association with DNA on the slowing of the migration of a counterion. The dashed line denotes the maximum MSD that a transiently adsorbed counterion can migrate. The dotted and long-short dashed lines denoted by t = 191 and 811 ps represent the MSD a free counterion would have migrated in the corresponding time durations, respectively. The longer the adsorption time, the larger the difference between adsorbed counterion and the free counterion and, consequently, the larger the effect.

the forces experienced by DNA. Continued strong interest in accurately determining the counterion condensation has led to new techniques. A buffer equilibration−atomic emission spectroscopy experiment (BE-AES)[57] reported charge neutralization values 76−87% for ion concentrations between 0.005 and 1.0 M, and an anomalous small-angle X-ray scattering (ASAXS) experiment gave the value 68%.[58]

III.6. Effect of Counterion Association on Migration. To illustrate the effect of the counterion association with DNA and the implication of the residence time on diffusion, we plot in Figure 8 the mean square displacement (MSD) for counterions in 10 nm open pores at the ion concentration 548 mM, which represents free counterion diffusion without association with the DNA. The MSD corresponds to the diffusion coefficient 1.756×10^{-5} cm^2/s, which is fairly representative of ion diffusion in open pore, as the concentration dependence of the diffusion coefficient is weak in the absence of DNA (see Figure 1). The horizontal dashed line at 0.54 nm^2 in the figure indicates the maximum MSD that a counterion bound to a DNA charge can migrate. The dotted line marked with τ_R = 191 ps and the long-short dashed line marked with τ_R = 811 ps indicate the MSD a free counterion would have migrated in the time duration the counterion is being adsorbed at 787 and 1 mM, respectively. The differences in MSD between the dotted line and the dashed line, and between the long-short dashed line and the dashed line represent the delaying effect of the DNA. Thus, at high ion concentration, C = 787 mM, for example, when the residence time of the counterion is relatively short (τ_R = 191 ps), a free counterion would migrate a mean square distance about 0.70 nm^2, whereas a counterion adsorbed to DNA could migrate a maximum mean square distance of R^2 = 0.54 nm^2. The free and the bound counterion MSD values are not significantly different, so the effect of the DNA−counterion association on the ion mobility is relatively minor. On the other hand, when the residence time is much longer, such as for a counterion at very low ion concentration, 1 mM (τ_R = 811 ps), a free counterion would have migrated a mean square distance about 2.9 nm^2 in the time duration, corresponding to a much higher mobility. However, in the same time duration a bound counterion can only migrate a maximum MSD 0.54 nm^2.

As a demonstration of the concept discussed above, we give a rough estimate of the counterion diffusion coefficient at 1 mM in a nanopore in the presence of DNA. The MSD 0.54 nm^2 in the time duration τ_R = 811 ps would yield an effective diffusion coefficient 3.33×10^{-6} cm^2/s, which is significantly smaller than the calculated diffusion coefficient of 6.93×10^{-6} cm^2/s from simulation, the reason being that there is also a contribution from the counterions that are not adsorbed to the DNA and that can remain free for quite a long time. On the basis of the discussion on counterion condensation in Section III.5, if we assume 25% of the counterions are free at any moment with a diffusion coefficient of 1.957×10^{-5} cm^2/s (bulk experimental value),[51] then the effective diffusion coefficient at 1 mM ion concentration would be $(3.33 \times 10^{-6}\,(75\%) + 1.957 \times 10^{-5}(25\%)) = 0.739 \times 10^{-5}$ cm^2/s, which is somewhat larger than the value obtained from the simulation but not entirely unreasonable. Thus, on the basis of the knowledge we gained on the dynamics of DNA−counterion interaction, we can reasonably estimate the plateau value D_{ads} in eqs 2a and 2b. The high concentration value D_{free} in eqs 2a and 2b can be taken as the open pore diffusion coefficient. This would then allow us to estimate the counterion diffusion coefficient in the entire concentration range.

IV. CONCLUSIONS

We have investigated the dynamics of the ion self-diffusion in a nanopore in the presence of DNA. We find that the diffusion coefficient of the co-ions is essentially unaffected by the DNA, whereas that of the counterions is strongly reduced by the DNA through the charge−charge interaction between the counterions and the DNA. Such a reduction is dependent on the ion concentration, resulting in significantly reduced diffusion coefficients at low concentrations, eventually reaching a plateau in the near absence of co-ions. The variation of the self-diffusion coefficients of the counterions can be quantitatively described by considering two contributions: one by the free diffusing counterions and the other by the transiently adsorbed counterions.

We examined in detail the dynamics of the transient counterion adsorption to and desorption from DNA over a range of ion concentrations, which are characterized by concentration dependent residence times that provide characteristic time scales for the process of ion exchange between the DNA and the environment. It is found that the residence time for the counterions to remain adsorbed to the DNA decreases with the ion concentration, whereas that for the counterions to remain free of DNA influence increases with the ion concentration. This is consistent with the physical mechanism that increased ion concentration provides stronger electric screening, which weakens DNA−counterion interaction so that the counterions are less attracted to the DNA. The residence time for the free counterions, that is, the time duration to migrate freely without the hindrance by DNA, besides the influence of the ion concentration, is largely determined by the pore volume and the ratio between the number of counterions and the number of DNA charge sites.

■ ACKNOWLEDGMENT

The work is supported by a grant from the NIH under Contract No. R01 HG002647-03. The author would like to

thank Dr. J. M. Ramsey and his group for many useful discussions during the course of this work.

REFERENCES

(1) Kasianowicz, J. J.; Brandin, E.; Branton, D.; Deamer, D. W. *Proc. Natl. Acad. Sci. U.S.A.* **1996**, *93*, 13770.
(2) Song, L. Z.; Hobaugh, M. R.; Shustak, C.; Cheley, S.; Bayley, H.; Gouaux, J. E. *Science* **1996**, *274*, 1859.
(3) Akeson, M.; Branton, D.; Kasianowicz, J. J.; Brandin, E.; Deamer, D. W. *Biophys. J.* **1999**, *77*, 3227.
(4) Meller, A.; Nivon, L.; Brandin, E.; Golovchenko, J.; Branton, D. *Proc. Natl. Acad. Sci.* **2000**, *97*, 1079.
(5) Menard, L. D.; Ramsey, J. M. *Nano Lett.* **2011**, *11*, 512.
(6) Fan, R.; Karnik, R.; Yue, M.; Li, D.; Majumdar, A.; Yang, P. *Nano Lett.* **2005**, *5*, 1633.
(7) Smeets, R. M. M.; Keyser, U. F.; Krapf, D.; Wu, M.-Y.; Dekker, N. H.; Dekker, C. *Nano Lett.* **2006**, *6*, 89.
(8) Liang, X.; Chou, S. Y. *Nano Lett.* **2008**, *8*, 1472.
(9) Chang, H.; Kosari, F.; Andreadakis, G.; Alam, M. A.; Vasmatzis, G.; Bashir, R. *Nano Lett.* **2004**, *4*, 1551.
(10) Manning, G. S. *Q. Rev. Biophys.* **1978**, *11*, 179.
(11) Jayaram, B.; Beveridge, D. L. *Annu. Rev. Biophys. Biomol. Struct.* **1996**, *25*, 367.
(12) Padmanabhan, S.; Richey, B.; Anderson, C. F.; Record, J. M. T. *Biochemistry* **1988**, *27*, 4367.
(13) Schellman, J. A.; Stigter, D. *Biopolymers* **1977**, *16*, 1415.
(14) Stellwagen, E.; Stellwagen, N. C. *Biophys. J.* **2003**, *84*, 1855.
(15) Keyser, U. F.; Koeleman, B. N.; Krapf, D.; Smeets, R. M. M.; Lemay, S. G.; Dekker, N. H.; Dekker, C. *Nat. Phys.* **2006**, *2*, 473.
(16) Cui, S. T. *J. Phys. Chem. B* **2010**, *114*, 2015–2022.
(17) Cui, S. T. *Phys. Rev. Lett.* **2007**, *98*, 138101.
(18) McQuarrie, D. A. *Statistical Mechanics*; Harper Collins Publishers: New York, 1976.
(19) Adamson, A. W.; Gast, A. P. *Physical Chemistry of Surfaces*, 6th ed., John Wiley and Sons: New York, 1997.
(20) Hunter, R. J. *Foundations of Colloid Science*; Clarendon Press: Oxford, 1987.
(21) Manning, G. S. *J. Chem. Phys.* **1969**, *51*, 924.
(22) Gelbart, W. M.; Bruinsma, R. F.; Pincus, P. A.; Parsegian, V. A. *Phys. Today* **2000**, *53*, 38.
(23) Wong, G. C. L. *Curr. Opin. Colloid Interface Sci.* **2006**, *11*, 310.
(24) Korolev, N.; Lyubartsev, A. P.; Nordenskiöld, L. *Adv. Colloid Interface Sci.* **2010**, *158*, 32.
(25) Montoro, J. C. G.; Abascal, J. L. F. *J. Chem. Phys.* **1995**, *103*, 8273.
(26) Honig, B.; Nicholls, A. *Science* **1995**, *268*, 1144.
(27) Ponomarev, S. Y.; Thayer, K. M.; Beveridge, D. L. *Proc. Natl. Acad. Sci.* **2004**, *101*, 14771.
(28) Feig, M.; Pettitt, B. M. *Biophys. J.* **1999**, *77*, 1769.
(29) Savelyev, A.; Papoian, G. A. *J. Am. Chem. Soc.* **2006**, *128*, 14506.
(30) Kirmizialtin, S.; Elber, R. *J. Phys. Chem. B* **2010**, *114*, 8207.
(31) Luan, B.; Aksimentiev, A. *Soft Matter* **2010**, *6*, 243.
(32) Maffeo, C.; et al. *Phys. Rev. Lett.* **2010**, *105*, 158101.
(33) Luan, B.; Aksimentiev, A. *Phys. Rev. E: Stat., Nonlinear, Soft Matter Phys.* **2008**, *78*, 021912.
(34) Aksimentiev, A.; Heng, J. B.; Timp, G.; Schulten, K. *Biophys. J.* **2004**, *87*, 2086.
(35) Aksimentiev, A. *Nanoscale* **2010**, *2*, 468.
(36) Ermak, D. L. *J. Chem. Phys.* **1975**, *62*, 4189.
(37) Ermak, D. L. A computer simulation of charged particles in solution. II. Polyion diffusion coefficient. *J. Chem. Phys.* **1975**, *62*, 4197.
(38) Allen, M. P.; Tildesley, D. J. *Computer Simulation of Liquids*; Oxford University Press: Oxford, 1987.
(39) Dang, L. X.; Kollman, P. A. *J. Phys. Chem.* **1995**, *99*, 55.
(40) Young, M. A.; Jayaram, B.; Beveridge, D. L. *J. Phys. Chem. B* **1998**, *102*, 7666–7669.
(41) Lamm, G.; Pack, G. R. *J. Phys. Chem.* **1997**, *101*, 959–965.
(42) Hingerty, B. E.; Ritchie, R. H.; Ferrell, T. L.; Turner, J. E. *Biopolymers* **1985**, *24*, 427–439.
(43) Beckstein, O.; Tai, K.; Sansom, M. S. P. *J. Am. Chem. Soc.* **2004**, *126*, 14694.
(44) Cruz-Chu, E. R.; Aksimentiev, A.; Schulten, K. *J. Phys. Chem. C* **2009**, *113*, 1850.
(45) Cui, S. T. *J. Chem. Phys.* **2005**, *123*, 054706.
(46) Boda, D.; Busath, D. D.; Henderson, D.; Sokolowski, S. *J. Phys. Chem. B* **2000**, *104*, 8903.
(47) Onsager, L.; Fuoss, R. M. *J. Phys. Chem.* **1932**, *36*, 2689.
(48) Jardat, M.; Turq, P. *Z. Phys. Chem.* **2004**, *218*, 699.
(49) Jardat, M.; Bernard, O.; Turq, P. *J. Chem. Phys.* **1999**, *110*, 7993.
(50) Jardat, M.; Hribar-Leeb, B.; Vlachy, V. *Phys. Chem. Chem. Phys.* **2008**, *10*, 449.
(51) Lide, D. R. *CRC Handbook of Chemistry and Physics*, 89th ed.; 2008−2009. Online at http://www.hbcpnetbase.com/.
(52) van Dam, L.; Lyubartsev, A. P.; Laaksonen, A.; Nordenskiold, L. *J. Phys. Chem. B* **1998**, *102*, 10636.
(53) Lee, S. H.; Rasaiah, J. C. *J. Phys. Chem.* **1996**, *100*, 1420.
(54) Koneshan, S.; Rasaiah, J. C.; Lynden-Bell, R. M.; Lee, S. H. *J. Phys. Chem. B* **1998**, *102*, 4193.
(55) Van Dorp, S.; Keyser, U. F.; Dekker, N. H.; Dekker, C.; Lemay, S. G. *Nat. Phys.* **2009**, *5*, 347.
(56) Ghosal, S. *Phys. Rev. E: Stat., Nonlinear, Soft Matter Phys.* **2007**, *76*, 061916.
(57) Bai, Y.; Greenfeld, M.; Travers, K. J.; Chu, V. B.; Lipfert, J.; Doniach, S.; Herschlag, D. *J. Am. Chem. Soc.* **2007**, *129*, 14981.
(58) Pabit, S. A.; Meisburger, S. P.; Li, L.; Blose, J. M.; Jones, C. D.; Pollack, L. *J. Am. Chem. Soc.* **2010**, *132*, 16334.